

A study of jets from b quarks produced in $e^+ e^-$ annihilations at $\sqrt{s} = 35 - 46$ GeV

TASSO Collaboration

W. Braunschweig, R. Gerhards, F.J. Kirschfink, H.-U. Martyn

I. Physikalisches Institut der RWTH Aachen,
Federal Republic of Germany^a

B. Bock¹, H.M. Fischer, H. Hartmann, J. Hartmann,
E. Hilger, A. Jocksch, R. Wedemeyer

Physikalisches Institut der Universität Bonn,
Federal Republic of Germany^a

B. Foster, A.J. Martin, A.J. Sephton

H.H. Wills Physics Laboratory, University of Bristol,
Bristol, UK^b

E. Bernardi, J. Chwastowski², A. Eskreys³,
K. Gather, K. Genser⁴, H. Hultschig, P. Joos,
H. Kowalski, A. Ladage, B. Löhr, D. Lüke,
P. Mättig⁵, D. Notz, J. Pawlak⁶, K.-U. Pösnecker,
E. Ros, W. Schütte, D. Trines, R. Walczak⁴,
G. Wolf

Deutsches Elektronen-Synchrotron DESY, Hamburg,
Federal Republic of Germany

H. Kolanoski

Physikalisches Institut, Universität Dortmund,
Federal Republic of Germany^a

T. Kracht⁷, J. Krüger, E. Lohrmann, G. Poelz,
W. Zeuner

II. Institut für Experimentalphysik der Universität
Hamburg, Federal Republic of Germany^a

A.T. Belk, D.M. Binnie, J.F. Hassard, J. Shulman,
D. Su⁸

Department of Physics, Imperial College, London, UK^b

F. Barreiro, A. Leites, J. del Peso

Universidad Autonoma de Madrid, Madrid, Spain^c

C. Balkwill, M.G. Bowler, P.N. Burrows,
R.J. Cashmore, G.P. Heath, P. Ratoff, I.M. Silvester,
I. Tomalin⁹, M.E. Veitch, J.M. Yelton¹⁰

Department of Nuclear Physics, Oxford University, Oxford, UK^b

S.L. Lloyd

Department of Physics, Queen Mary College, London, UK^b

G.E. Forden¹¹, J.C. Hart, D.H. Saxon

Rutherford Appleton Laboratory, Chilton, Didcot, UK^b

S. Brandt, M. Holder, L. Labarga¹²

Fachbereich Physik der Universität-Gesamthochschule Siegen,
Federal Republic of Germany^a

Y. Eisenberg, U. Karshon, G. Mikenberg,
A. Montag, D. Revel, E. Ronat, A. Shapira,
N. Wainer, G. Yekutieli

Weizmann Institute, Rehovot, Israel^d

D. Muller, S. Ritz, D. Strom¹³, M. Takashima, Sau
Lan Wu, G. Zoernig

Department of Physics, University of Wisconsin, Madison, WI,
USA^e

Received 23 August 1988; in revised form 8 October 1988

¹ Now at Krupp Atlas Electr. GmbH, Bremen FRG

² On leave from Inst. of Nuclear Physics, Cracow, Poland

³ Now at Inst. of Nuclear Physics, Cracow, Poland

⁴ Now at Warsaw University, Poland

⁵ Now at IPP Canada, Carleton University, Ottawa, Canada

⁶ On leave from Warsaw University, Poland. Partially supported
by grant CPBP 0.106

⁷ Now at Hasylab, DESY, Hamburg, FRG

⁸ Now at Rutherford Appleton Laboratory, Didcot, Oxon, UK

⁹ Now at Imperial College, London, UK

¹⁰ Now at University of Florida, Gainesville, FL 32611, USA

¹¹ Now at SUNY Stony Brook, Stony Brook, NY, USA

¹² Now at SLAC, Stanford, California, USA

¹³ Now at University of Chicago, Chicago, Illinois, USA

^a Supported by Bundesministerium für Forschung und Technologie

^b Supported by UK Science and Engineering Research Council

^c Supported by CAICYT

^d Supported by the Minerva Gesellschaft für Forschung GmbH

^e Supported by US Dept of Energy, contract DE-AC02-76ER000881 and by US Nat. Sci. Foundation Grant no INT-8313994 for travel

Abstract. A b enrichment technique using the long B lifetime has been developed, by which ~ 600 hadronic events with $>65\%$ b purity are obtained. The properties of the associated jets are studied, with comparisons made between them and those in hadronic data in which b quarks make up only 10% of the total, and jets in Monte Carlo events. The distributions in rapidity and multiplicity yield two new determinations of the fragmentation variable z for b hadrons and confirm that the b fragmentation function is hard. We also present the first measurement of the relative strength of the strong interaction coupling of the b quark compared with the average of all flavours.

1 Introduction

This paper introduces a method of isolating large samples of hadronic events with high b quark content by using the relatively long flight path of B hadrons: recognition of secondary vertex structure associated with the B decay is used as a tag [1]. The systematic effects of this method are very different from those associated with the more usual lepton tag technique [2]. The properties of jets of hadrons produced by initial b quarks are extracted and compared with the properties of average jets. Both the rapidity and multiplicity distributions for the B jets are sensitive to the b fragmentation function and the mean value of the fragmentation variable z has been determined. The first measurement of the ratio of coupling constants $\frac{\alpha_s(b)}{\alpha_s(\text{average})}$ is presented. This technique of vertex tagging will be increasingly powerful at higher energies.

This study used the TASSO detector of which a detailed description can be found in [3]. Central to this analysis are the TASSO Vertex Detector, the VXD [4], which is described in more detail in the next section and the TASSO main drift chamber [5]. The 45 pb^{-1} of data taken by TASSO in 1983–1985, at centre of mass energies of 38–46 GeV contain a total of 7983 hadronic events. The 110 pb^{-1} data taken in 1986 at a fixed energy of $\sqrt{s}=35 \text{ GeV}$ amount to 31 176 hadronic events which passed standard hadronic selection cuts [6]. The same analysis method is used for both data samples and most of the discussion will be based on the analysis of the large sample of 35 GeV data, but results from the high energy data are given where relevant.

2 The vertex detector

The main features of the VXD which are important to this analysis are summarised here. The VXD had

8 sense layers between radii of 8.1 cm and 14.9 cm and an active length of 57.2 cm. The materials in the beam pipe and assemblies within the VXD active volume, including the 95/5 Ar/CO₂ gas mixture, amounted to 0.9% of a radiation length. The chamber spatial resolution for hadronic tracks was found to be $\sim 110 \mu\text{m}$ with a $\pm 25\%$ variation depending on the layer and cell position of the hit. The distribution of the distance of closest approach of a reconstructed track to the interaction point depends sensitively on the track momentum especially for tracks below 1 GeV/c, due to multiple scattering. A study of high energy wide angle back-to-back two-prong events yielded an individual track impact parameter resolution of $\sim 100 \mu\text{m}$. This agrees very well with the value obtained from Monte Carlo Bhabha events.

The tracks used in this analysis were those found by the track finder FELIX [7] and were refitted [8] in the plane perpendicular to the beams – the $r-\phi$ plane – allowing for a single kink due to multiple scattering between the main drift chamber and VXD.

3 Monte Carlo modelling

The evaluation of data presupposes an understanding of the experimental acceptances and biases and of the theoretical kinematics of the process under consideration. The vertex tagging method is very sensitive to the B decay multiplicity and, to a lesser extent, to the b fragmentation function. In order to estimate backgrounds in the b -enriched sample, we used a Monte Carlo generator containing a B decay routine tuned to reproduce the results of CLEO [9] and with a b fragmentation function which could be easily adjusted without affecting properties of jets initiated by other quarks.

The Monte Carlo used in this analysis incorporated independent jet fragmentation [10] with the extended FKSS [11] calculation of the full second order QCD matrix element. The B decay Monte Carlo reproduced the results of CLEO and the fragmentation functions for the heavy quarks were represented by the single parameter form of Peterson et al. [12]. The production of charm and bottom baryons was not simulated, but they would be expected to have little influence on this analysis. In the Monte Carlo, the B lifetime was set to be 1.23 ps and the average value of the b fragmentation function, $\langle z_b \rangle$ was taken as 0.80, except where stated otherwise. Table 1 lists the important parameters of the Monte Carlo. The TASSO Drift Chamber (DC) and VXD were simulated with efficiency and resolution parameters tuned to values obtained in hadronic data. Noise hits in the detector were taken from random beam crossing events in the data. The Monte Carlo events were sub-

Table 1. Main parameters used in the Monte Carlo (QCDF at $W = 35$ GeV)

QCD matrix element calculation			
Extended FKSS full 2nd order	$\varepsilon = 0.2 \cdot E_{\text{beam}}, \delta = 40^\circ$		
Independent jet fragmentation model			
$\alpha_s = 0.155$	$\sigma_q = 0.350$ GeV		
EP conservation [26]			
Light quark fragmentation $\alpha(1-z)^{z_L}$	$\alpha_L = 0.660$		
Heavy quark fragmentation [12]	$\varepsilon_b = 0.010, \varepsilon_b = 0.075$		
$P/(P+V)$	$qqq/(qq+qqq)$	$u\bar{u}:d\bar{d}:s\bar{s}$	
0.42	0.10	1:1:0.4	
Heavy meson lifetimes (ps)			
$\langle B \rangle$	D^0	D^+	D_s
1.23	0.43	1.03	0.35

ject to the same processing procedure as for the data, including the track finding.

Among the most successful Monte Carlo generators are those of the Lund group [13] embodying either second order QCD or a leading logarithm QCD cascade. In the latest and best studied versions, the partons are connected with a string, and fragmented with a universal form for the fragmentation function. We have not used these generators for the bulk of our work for two reasons. First, the B decay routine embedded in them has not been tuned to reproduce the $\Upsilon(4S)$ results. Secondly, the universal symmetric fragmentation form yields a very hard fragmentation function, which cannot be tuned independently of other variables.

4 The b -enrichment technique

The tagging method depends on our finding the event vertex, then finding characteristic vertices associated with the decay of a particle relative to this event vertex. Since the resolution in the TASSO $r-\phi$ plane is an order of magnitude better than in the plane containing the track and the beams – the $s-z$ view – all distance variables refer to projected distances in the $r-\phi$ plane. Only charged tracks are considered.

4.1 Event vertex finding

The vertex tagging method depends on the separation of B decay vertices from the interaction point. The interaction region – the beam spot – is relatively large and individual events can occur within an envelope about the mean beam position. The profile and centre

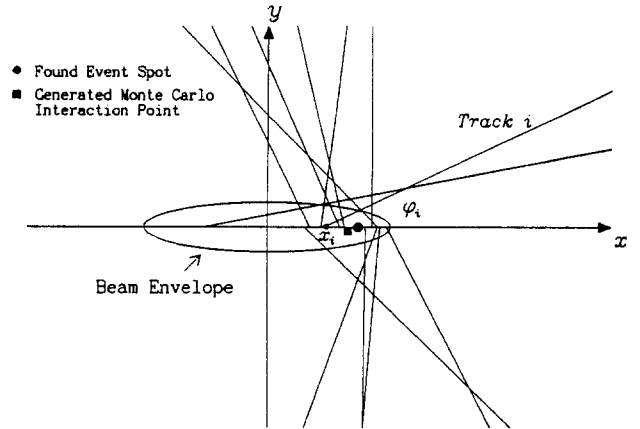


Fig. 1. Illustration of event spot finding scheme for a single Monte Carlo event. The event spot is reconstructed from the weighted positions of the event tracks i on crossing the x axis

of the beam spot were determined for each data taking run, or for a few runs grouped together when event statistics dictated, using beam associated events [14]. The statistical errors for the beam centre coordinates were typically $\pm 35 \mu\text{m}$ in the 1986 data. The track resolution gave the major contribution to the error in the beam y position determination where the expected beam ‘height’ is of order $20 \mu\text{m}$, while the error in the beam centre x coordinate is insignificant compared with the beam envelope size of $\sim 350 \mu\text{m}$. Here, both x and y are perpendicular to the beam, with positive y vertically upwards, and positive x towards the storage ring centre.

It is possible to determine the actual interaction point for an event more accurately by exploiting the fact that the vertical spread in y is about ten times smaller than the lateral spread in x . With the event vertex y coordinate fixed to that of the beam centre, the crossing points x_i , of all good quality tracks i (as defined below) in an event with the horizontal line $y = y_{\text{beam}}$ were found and weighted by $W_i = |\sin \phi_i|$ to account for the fact that the vertical tracks provided more accurate crossing points in x . Given the sum of the weights for all tracks, W_0 , an ordered sum of track weights was then made in the order of increasing x_i , until the sum reached the point closest to $W_0/2$. The weighted average of the two x_i points just above and just below this half-sum was then assigned as the estimated event spot x . Notice that biasing by any single track is avoided. The resolution on the resulting x coordinate, obtained from Monte Carlo, is $\sim 200 \mu\text{m}$. The procedure is illustrated in Fig. 1, which represents a single Monte Carlo event. This procedure was found not to be biased for or against finding Monte Carlo b decay events.

4.2 Event and track selections

Events were selected from standard hadronic events [6] according to the following criteria:

- $|\cos \theta_{\text{thrust}}| < 0.75$ to avoid the worst of acceptance limitations.
- Events in runs with a poorly determined beam spot were rejected.
- Events with large clusters of noise hits in the VXD were rejected.
- Events which failed a minimum weight requirement of $W_0 > 3$ in the event spot finding procedure were rejected.

There were 21322 events at $\sqrt{s} = 35$ GeV surviving the selection cuts and 5734 events for the high energy data. Tracks found by the FELIX track finder were subjected to the following track quality cuts before being used in the tagging procedure:

- $\chi^2_{r-\phi}/\text{NDF} < 3.0$
- $|\cos \theta| < 0.87$
- $|z_0| < 10.0$ cm
- $|d_0| < 0.20$ cm
- $P > 0.3$ GeV/c
- Number of VXD hits on track ≥ 4

where d_0 is the perpendicular distance of a track, measured from the reconstructed interaction point, in the $r-\phi$ plane and z_0 is the distance along the beam axis of the point associated with that d_0 projected perpendicularly onto the beam axis.

The last 3 cuts are the most important for rejecting spurious tracks or K^0 , A decay tracks and limiting the effect of multiple scattering.

4.3 Tagging method

No attempt has been made to reconstruct a multi-track b decay vertex. Rather, secondary decay structures were identified by a method in which we considered all pairs of tracks, satisfying the criteria below, in turn. A vertex was constructed from each such pair, the distance l_v from the vertex was found and the angle α between the sum of the two-track momenta and the line going through the event vertex and the two track vertex was reconstructed. The distance l_v and $\cos \alpha$ were used to assign a weight to the vertex. Both l_v and the impact parameter were defined in the $r-\phi$ plane. The definitions of various vertex geometry parameters are illustrated in Fig. 2.

The following cuts were used to reject spurious vertices or vertices unlikely to come from a pair of B decay tracks:

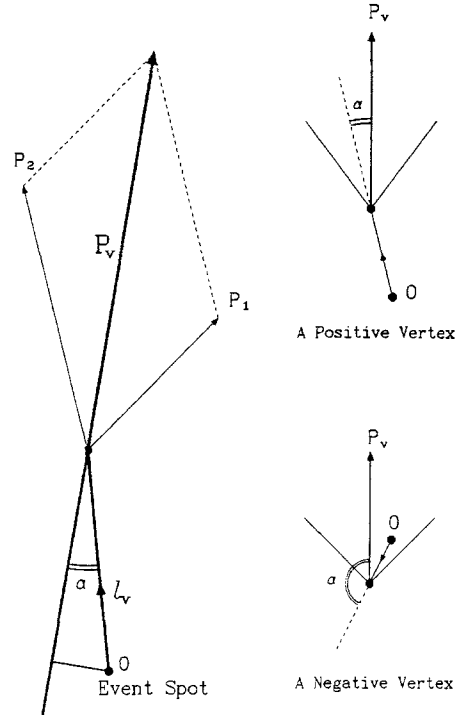


Fig. 2. Illustration of geometry parameters used in vertex weight definition. P_1 , P_2 and P_v are the tracks' and resultant vertex momenta

$$\begin{aligned} \Psi_{3D} &< 60^\circ \\ \Psi_{2D} &5^\circ \\ l_v &< 7 \text{ mm} \end{aligned}$$

where Ψ_{3D} and Ψ_{2D} are the opening angles between the momentum vectors of the 2 tracks in 3-D and 2-D (that is, the $r-\phi$ plane) respectively.

Each surviving vertex was then weighted by an amount which reflected its likelihood of having come from a secondary decay. A study of the decay kinematics, and of effects such as multiple scattering, suggested the empirical form:

$$W = \left(1 - e^{-\frac{(l_v \cos \alpha)^2}{2\sigma_v^2}}\right) \cdot \cos \alpha. \quad (1)$$

The vertex distance resolution parameter σ_v was calculated from the momentum dependent track impact parameter resolution obtained in Monte Carlo studies together with the track opening angles and folded in quadrature with an event vertex resolution of 200 μm .

The event tag is made on the sum of the weights of all two track vertices as defined above. This definition ensures that vertices formed from a pair of fragmentation tracks, originating at the interaction point, are equally likely to contribute positive or negative weights to the sum. Events originating with primary

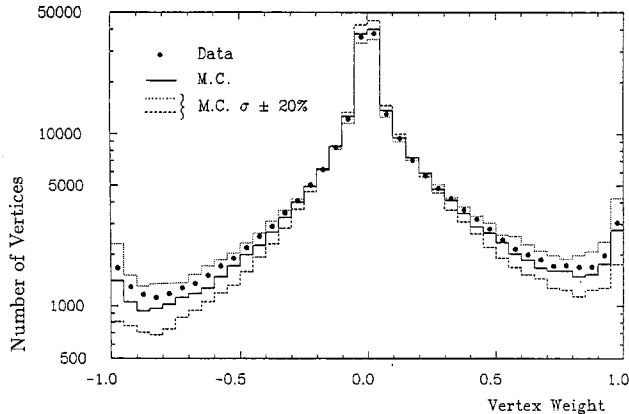


Fig. 3. Normalised distributions of vertex weights for all accepted pairs of tracks. The Monte Carlo distribution is shown for comparison, as are the distributions in which the Monte Carlo resolution σ of the track impact parameter resolution is smeared by $\pm 20\%$

u , d or s quarks are thereby suppressed. Notice that the maximum obtainable weight is 1, and that spurious vertices with their momentum vectors nearly perpendicular to the apparent decay paths are suppressed by the factor $\cos \alpha$.

Events are tagged by imposing a cut on the summed weights $\sum W$ of two-particle vertices and two modes of tagging were used. In the *jet-mode tag* an event is divided into 2 hemispheres, using the plane perpendicular to the event thrust axis so that tagging one side would leave the other half to be studied relatively free of bias. In the *global-mode* all track pairs in an event are taken without dividing the event. The cut on pair opening angle ensures that few pairs are accepted where the tracks are drawn from different hemispheres thereby restricting the otherwise large number of spurious combinations. The *global-mode* is especially suitable for studying events with B mesons not produced back to back e.g. 3 or 4 jet events.

The normalised distribution of vertex weights is shown in Fig. 3 for all two track vertices which passed the selection cuts. This distribution is for track pairs within the same hemisphere with the event divided by a plane perpendicular to the event thrust axis. The variation of the weight with a $\pm 20\%$ change in assumed track impact parameter resolution in the Monte Carlo is also shown. Most of the vertices are distributed symmetrically around zero and their distribution is consistent with that expected from the broadening due to detector resolution. There is a significant excess of positive weights, as would result from the decay of long-lived particles.

The half event weight sums for the *jet-mode tag* are shown in Figs. 4 and 5 for data and Monte Carlo, normalised to the same number of input events. The flavour content in the Monte Carlo at positive $\sum W$

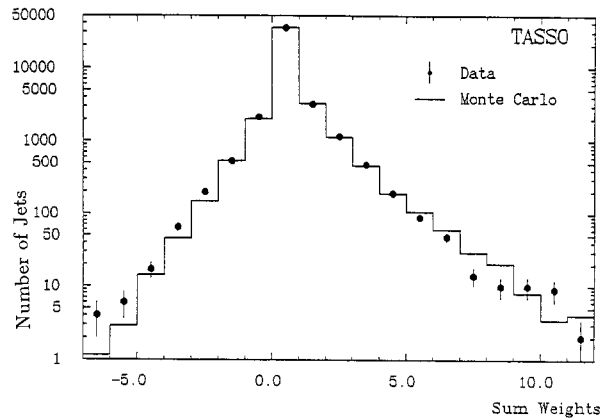


Fig. 4. Half event weight sums for jet-mode tag (whole range)

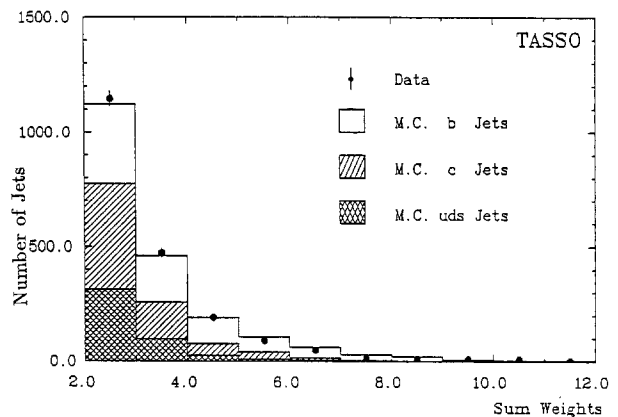


Fig. 5. Half event weight sums for jet-mode tag (positive tail)

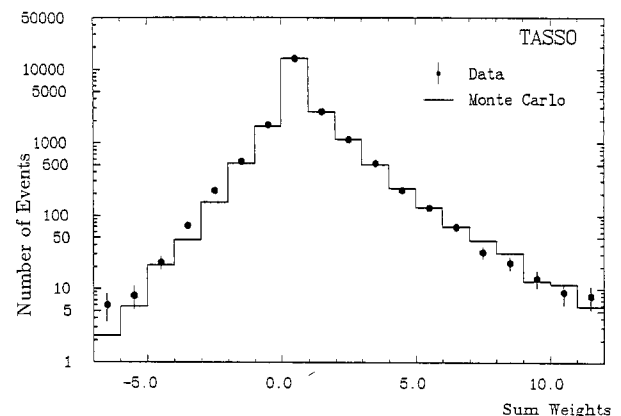


Fig. 6. Whole event weight sums for global-mode tag (whole range)

is also indicated. A similar set of plots for the *global-mode tag* can be found Figs. 6 and 7.

The enrichment in $b\bar{b}$ events can be obtained by various cuts on the weight sum $\sum W$ depending on the desired purity and efficiency. The cut selected for this analysis was $\sum W \geq 4$ for both tagging modes. Among the 21 322 inputs 35 GeV data events, the

Table 2. Purities and efficiencies of the tagging techniques

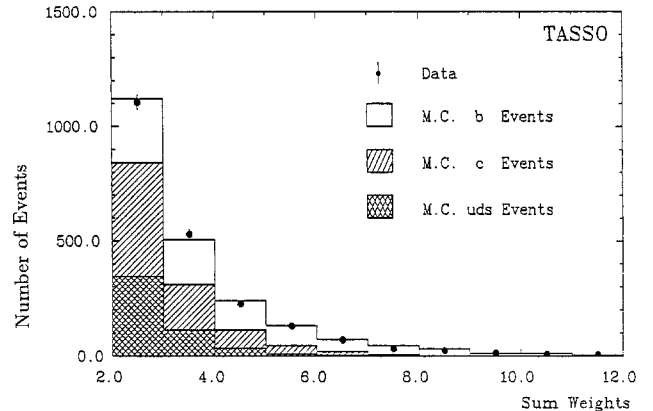
Tag mode	Tagged jets or events		Event Purity	Event tagging Efficiency
	Data	Monte Carlo		
Jet-mode	374 jets	431 jets	68%	11%
Global-mode	516 events	565 events	68%	16%

number of tagged jets/events and estimated b efficiency and purity are listed above in Table 2 for data and Monte Carlo with the Monte Carlo normalised to the same number of input events as in the data. The errors on these estimates are discussed in Sect. 5. The agreement between data and Monte Carlo is not perfect, but the discrepancies have little effect on the b purity of the enriched sample. If the discrepancies are real and are attributed wholly to the b tagging efficiency, then the b event efficiencies and purities inferred are 9% and 63% for the jet mode and 14% and 65% for the global mode. We note that using the Lund second order generator we find b tagging efficiencies and purities of 12% and 60% in the *jet-mode*, while the numbers of events initiated by u , d , s and c quarks which are tagged are in good agreement with those obtained from the independent jet generator. The above changes in purity are well within the estimates of systematic errors given in Sect. 5.

The most serious source of background is from the decay of charmed particles from events with primary c quarks. Monte Carlo studies show that this source is greatly suppressed (Figs. 4–7). The most important factor in this suppression is the average decay charged multiplicity of B mesons of ~ 5.5 , compared with ~ 2.4 in D decays.

The efficacy of this tagging method has been studied in several ways.

- The number of double tag events in the *jet-mode*, compared with the number of single jet tags with $\sum W \geq 3$, was 26 doubles out of 846 tagged jets, while the Monte Carlo predicted a rate of 30. One would expect 8 were the weights uncorrelated.
- We found that the mean track impact parameter opposite tagged jets was $93 \pm 19 \mu\text{m}$ in the data and $129 \pm 12 \mu\text{m}$ in the Monte Carlo which can be compared with $\sim 35 \mu\text{m}$ in the average jets.
- The ‘sphericity product’ method employed for the b enrichment in the TASSO B lifetime measurement [15], is based on event shape variables alone and thus is independent of the decay distance information used for vertex tagging. Following the standard cuts as in [15] to consider tracks within a 41° cone around the sphericity axis and using a Lorentz boost β of 0.70, the cut of $S_1 \cdot S_2 > 0.1$ gave a b purity of 33%

**Fig. 7.** Whole Event weight sums for global-mode tag (positive tail)

in the Monte Carlo. The number of events in the data passing both the $\sum W \geq 4$ cut in the *global-mode* vertex tagging and the cut $S_1 \cdot S_2 > 0.1$ was 175 (Monte Carlo predicting 198) while if there were no correlation between the two methods one would expect only 64 events.

All these results confirm the overall effectiveness of the tagging method.

5 Study of systematic effects

The results on systematic uncertainties given here are mainly obtained from the *jet-mode* tag; there are similar effects in both methods.

By running the tagging program on the rejected events with large noise hit clusters in the VXD, it was found that the overall tagging rate was similar to that of the normal sample. Thus the remaining effect due to small hit clusters remaining in the normal sample was deemed negligible. Similarly, possible uncertainties in event spot coordinates were found to cause immeasurably small changes in the b tagging efficiency or the b purity. No dependence in efficiency on the azimuthal angle ϕ of the event thrust axis was found.

The effect of a systematic misalignment of the VXD with respect to the main drift chamber was tested by artificially rotating the VXD by 0.1 mrad, and then refitting the tracks for all data events. Only 5% of the previously tagged candidates failed tagging cuts while a similar number of new candidates was

Table 3. Systematic error contributions in jet-mode Tag with $\sum W \geq 4$

Systematic error origins	No. of tagged jets		
	b	c	uds
Actual contents	255	80	39
Impact parameter resolutions	+31	+24	+12
	-27	-12	-5
Light flavour fragmentation model		+12	+17
		-9	-6
B lifetime	+44		
	-30		
B decay charge multiplicity	+18		
	-18		
b fragmentation function	-4		
	-28		
Charm fragmentation function		+9	
		-12	
Combined	+57	+28	+21
	-52	-19	-8

added. The change in b purity was again negligible. This rotational error is considered to be the positional misalignment which would have the greatest effect on b purity and efficiency.

We will now outline the way in which effects which are significant were studied. The results of these studies are in Table 3. The effect due to uncertainties in VXD resolution was studied by changing the track impact parameter resolution values in the Monte Carlo by $\pm 10\%$. A comparison of vertex weight distributions of data and Monte Carlo can be seen in Fig. 4.

We estimated the effect of uncertainties in the fragmentation modelling for the lighter flavour $udsc$ background by varying the vertex 3-D opening angle

cut from 55° to 66° and noting the change in the number of tagged lighter flavour events.

The effect of the uncertainty in B meson lifetime was found to be important. Monte Carlo jets were weighted with a broad range of B lifetime values and the resultant jet tagging efficiency and b purity values were noted for a fixed cut of $\sum W \geq 4$. The systematic error on the b content in the tagged sample was taken as that due to the variation of B lifetime between 1.0 and 1.4 ps.

The effect of the uncertainties in the b fragmentation function was studied using two extra samples of Monte Carlo b events generated with ε_b – the free fragmentation parameter – of 0.003 and 0.03, corresponding to 0.86 and 0.73 respectively in the average value $\langle z_b \rangle$ of the fragmentation function, again using the Peterson function. The former value, producing a harder function, made practically no difference; the number of tagged b 's was reduced by about 11% for the softer b fragmentation function. The uncertainties due to charm fragmentation were studied by weighting charm jets corresponding to an effective variation of ε_c from 0.03 to 0.13, equivalent to a variation in $\langle z_c \rangle$ of 0.73 to 0.60.

The variations of b content due to the uncertainty of B decay charged multiplicity was also included by considering the differences in efficiency and purity found for Monte Carlo b jets in the range $5.34 < \langle n_B \rangle < 5.80$.

The effect of uncertainties in D decay charged multiplicities was also checked and was found to be negligible. The dependence on primary D^0/D^+ yield was checked (bearing in mind their rather different lifetimes) and was also found to be undetectable.

We find that the uncertainty in B lifetime is the largest source of systematic error in flavour content. The uncertainties in detector resolution and the modelling of fragmentation also contribute significantly.

Table 4. Final estimates of flavour content in tagged data samples with statistical and systematic errors all included

Tagging mode		Tagged jets or events		
		b	c	uds
35 GeV data				
Jet-mode	No. of jets	255^{+59}_{-54}	80^{+29}_{-21}	39^{+22}_{-10}
	Flavour fractions	$68 \pm 7\%$	$21 \pm 6\%$	$11 \pm 4\%$
Global-mode	No. of events	349^{+76}_{-87}	120^{+42}_{-25}	47^{+26}_{-12}
	Flavour fractions	$68 \pm 7\%$	$23 \pm 6\%$	$9 \pm 4\%$
42 GeV data				
Jet-mode	No. of jets	72^{+23}_{-14}	26 ± 10	20 ± 8
	Flavour fractions	$61 \pm 10\%$	$22 \pm 8\%$	$17 \pm 7\%$
Global mode	No. of events	99^{+31}_{-18}	40 ± 14	25 ± 10
	Flavour fractions	$60 \pm 9\%$	$25 \pm 8\%$	$15 \pm 6\%$

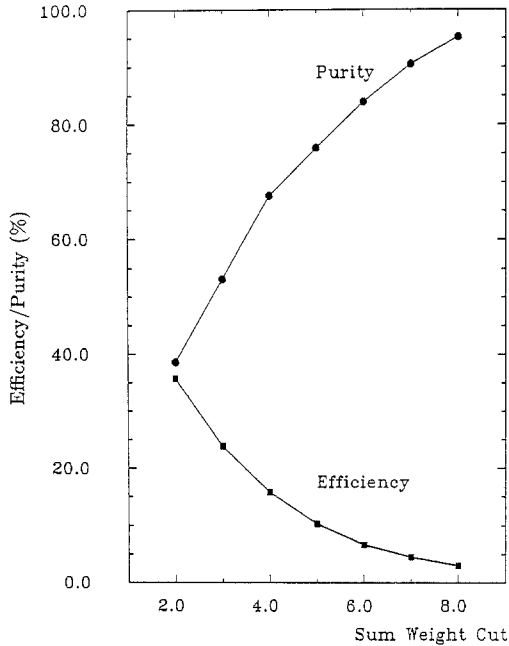


Fig. 8. Global-mode tag b purity and efficiency for different $\sum W$ cuts

The best estimates of flavour content in the tagged data sample with systematic errors and statistical errors added together are listed in Table 4 with a tagging cut of $\sum W \geq 4$ for both modes. The corresponding results for the high energy data are also listed. The most important point to be noted is that the efficiency of this first attempt on vertex tagging has already surpassed the best of the high P_T lepton tags [2]. The uncertainty of $\sim 7\%$ in b purity is also comparable to that of the high P_T lepton tag experiments.

The Monte Carlo estimates of b tagging efficiency and purity are plotted for the *global-mode* in Fig. 8 with different $\sum W$ cuts. It can be noted that a rather wide choice of efficiency and purity combinations are available for different analysis purposes.

Although this method has natural biases in favour of b events with long B decay times and large B decay charged multiplicities, and against B 's with very low momenta, it has a relatively uniform acceptance in momentum of B 's with momenta > 10 GeV/c, which makes it a particularly suitable method for the study of fragmentation functions.

6 The properties of jets from b -quarks

A relatively unbiased sample of b enriched jets can be obtained from those recoiling against the jet tagged in the *jet mode*. With $\sum W > 4$, our sample contained 374 tagged jets. To use this sample, correction factors accounting for QED radiative effects, detector accep-

tance and hadronic selection biases and their effects on both jet and track characteristics were determined by Monte Carlo. Except when otherwise stated, the distributions in tracks and jets have been thus corrected with Monte Carlo data at a nominal energy of 35 GeV. These results have been evaluated using the independent jet model Monte Carlo [10]. Where appropriate, that is, for studies of average jets, checks have been made with the Lund Monte Carlo [13].

6.1 Jet sphericity and thrust

The jet sphericity and thrust distributions for b enriched jets as compared with average jets and Monte Carlo are shown in Figs. 9 and 10 respectively. The

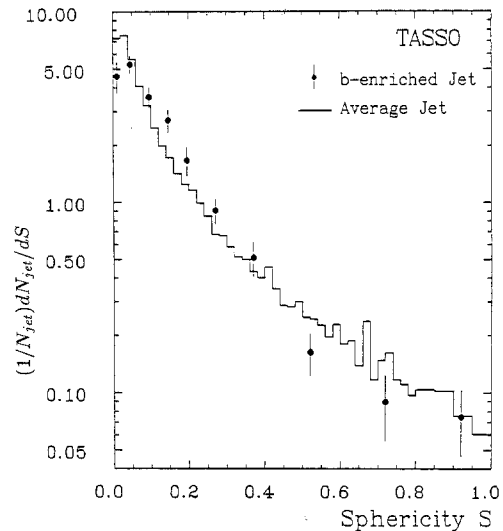


Fig. 9. Jet sphericity of b enriched and average jets

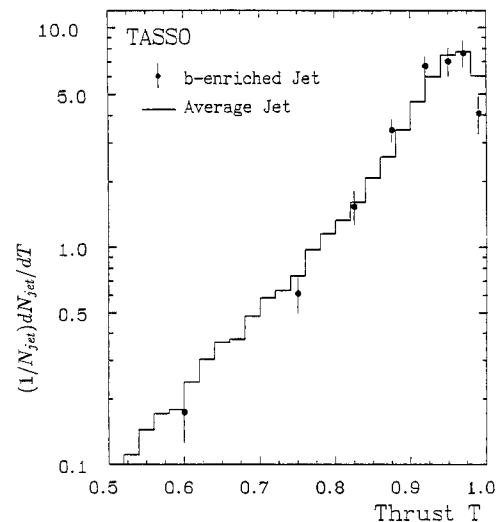


Fig. 10. Jet thrust of b enriched and average jets

sphericity and thrust were calculated using tracks in a hemisphere but using axes determined from tracks in the whole event.

The sphericity distribution is much broadened, and the thrust distributions noticeably so, for the b -enriched jets. This is to be expected because of the relatively low velocity of the b hadron, and the approximately 5.5 charged tracks per decay. However, this broadening effect does not extend to the very high sphericity and very low thrust tails where hard gluon emissions are expected to dominate.

6.2 Transverse and longitudinal momenta

The squared transverse momentum P_T^2 distributions and rapidity distributions for charged tracks in the b enriched jets are shown in Figs. 11 and 12 respectively. The P_T was defined with respect to the event sphericity axis and the $P_{||}$ used for calculating rapidity was with respect to the event thrust axis. All particles were assigned the pion mass.

The P_T^2 distributions were similar in b enriched jets and average jets. When P_T was defined with respect to the thrust axis, the distribution of b -enriched jets again closely follows that of average jets, in contrast to the P_T of leptons in semileptonic decays.

The difference in rapidity distribution, however, between the b enriched jets and average jets, is statistically significant. This difference lies primarily (Fig. 12) in an enhancement of the B jet rapidity in the mid-plateau region of $\eta \sim 1-3$. The tagged jets contain more tracks from B decay than do the enriched jets and the enhancement was found to be even more pronounced for the tagged jets in both data and Monte Carlo. Its origin is easily understood. A B decay pro-

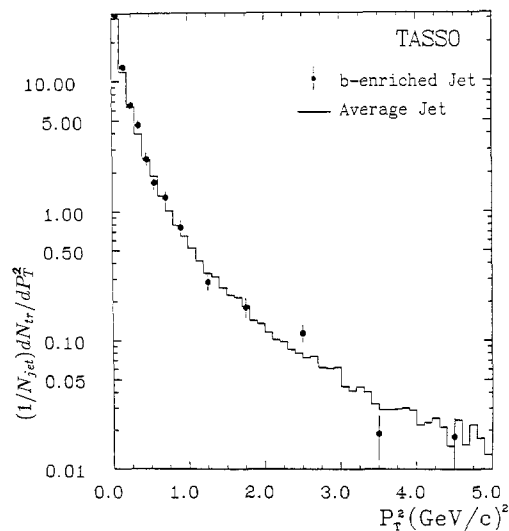


Fig. 11. Charged track jet P_T^2 in b enriched and average jets

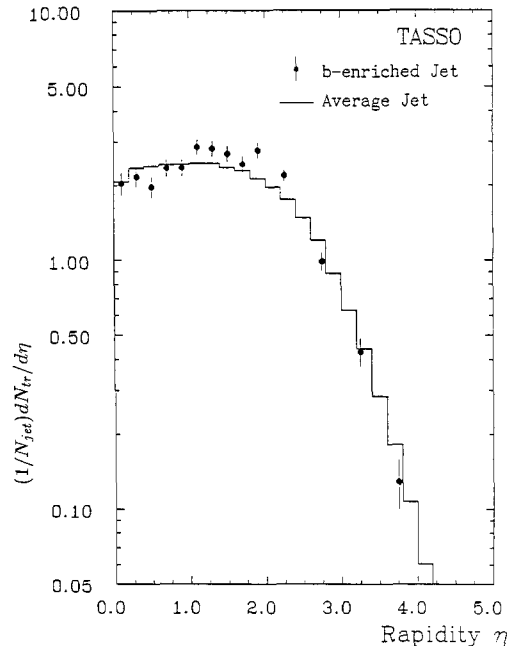


Fig. 12. Charged track rapidity in b enriched and average jets

vides on average 5.5 charged tracks in a B jet out of a total of about 8 (see Sect. 6.6) and these tracks are isotropically distributed in the B rest frame. In this frame the rapidity distribution of such tracks is peaked at zero and is forward-backward symmetric. This distribution is transformed to the laboratory frame merely by adding to the track rapidity the rapidity of the B meson. The distribution in rapidity is thus sensitive to the b fragmentation function, and we have used the rapidity distribution to determine the mean value of the fragmentation variable z for the b initiated jets.

The uncorrected rapidity distribution for the B enriched jets was compared with that for Monte Carlo events generated over a range of $\langle z_b \rangle$, using the Peterson function, which were passed through a simulation of the detector and the same jet tagging as the data. The quantity $\langle z_b \rangle$ is the average value of z_b , which is defined as

$$z_b = (E_b + p_b^{\parallel}) / (E_q + p_q)$$

where the suffixes b and q refer to the hadron and primary quark respectively, and the hadron momentum p_b^{\parallel} is the component measured parallel to the primary quark direction. The population of each rapidity bin in the Monte Carlo enriched jets was parametrised as a function of mean z_b and the data fitted. The data were well reproduced with a value of $\langle z_b \rangle$ of 0.85 and these studies yielded

$$\langle z_b \rangle = 0.85 \pm 0.03$$

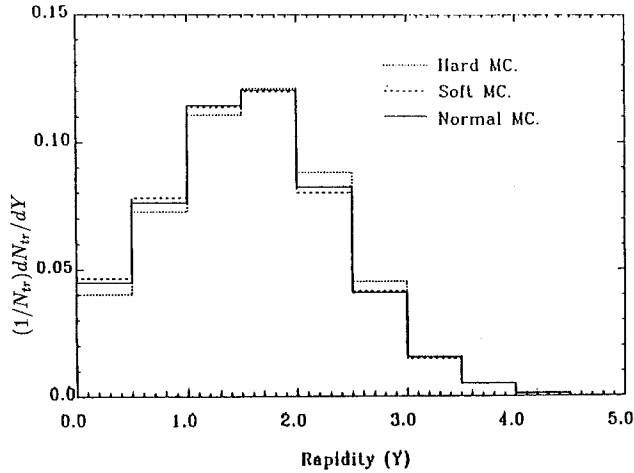


Fig. 13. The dependence of the rapidity distribution on the fragmentation function in b enriched jets

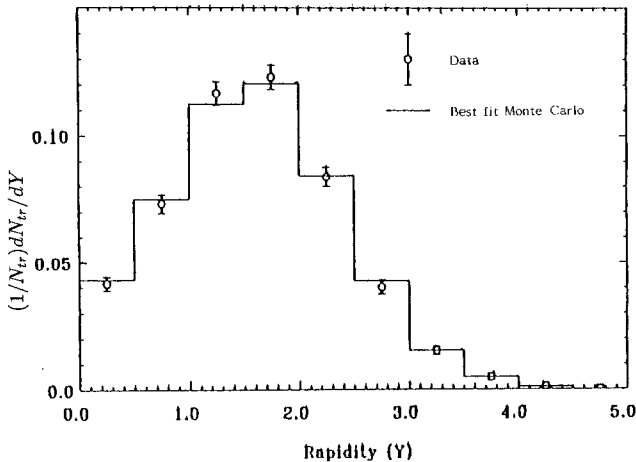


Fig. 14. Comparison in track rapidity between data and interpolated Monte Carlos

where the error is statistical only. The systematic error will be discussed later. This result is consistent with the results from prompt lepton analyses [16] and is independent of that method. Figure 13 shows the dependence of the rapidity distribution on the fragmentation function and Fig. 14 the comparison between the data and the interpolated Monte Carlo fragmentation distribution.

6.3 Inclusive momentum spectrum

The inclusive momenta of charged particles are shown in Fig. 15 for b enriched jets and average jets. Again, the softer momentum spectrum of the b jets can be seen from the excess of tracks in the low x region just below 0.2 for the b enriched jets compared with the average jets. This is a direct reflection of the rapid-

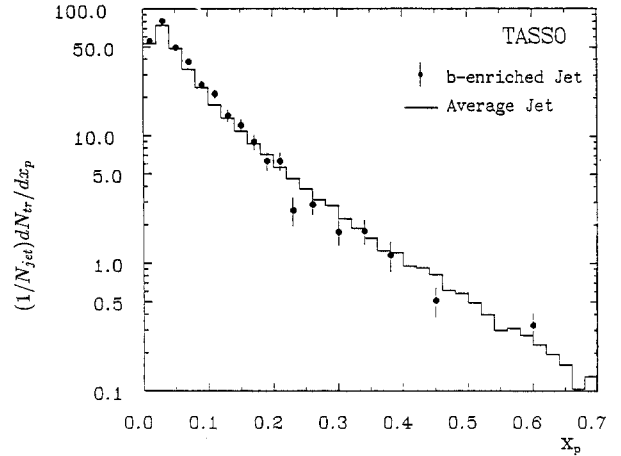


Fig. 15. Scaled momentum of charged tracks in b enriched and average jets

ity peak already discussed and is modelled successfully by the Monte Carlo.

6.4 Charged multiplicity

To take account of the charged multiplicity distributions' sensitivity to detector biases, the following procedure was taken to unfold the charged multiplicity distributions with the assistance of Monte Carlo. The first step was to correct the tracking inefficiency and the losses due to limited detector acceptance. This was done by checking the number of observed tracks N_T against the generated number of tracks for each Monte Carlo event after detector simulation and track finding. An unfolding matrix was formed to predict the probability that the true charged multiplicity of an event was n_p when n_o tracks were observed. An unfolded charged multiplicity distribution could be thereby obtained:

$$f(n_p) = \frac{1}{N_{ev}} \sum_{n_o} \varepsilon(n_p, n_o) N(n_o) \quad (2)$$

where

$$\varepsilon(n_p, n_o) = \frac{\text{No. of events with } n_p \text{ tracks produced when } n_o \text{ tracks were observed}}{\text{No. of events with } n_o \text{ tracks observed, } N(n_o)} \quad (3)$$

This procedure typically gave ~ 1.9 tracks more per event at $\sqrt{s} = 35$ GeV after unfolding compared with the observed tracks. The systematic uncertainty in the unfolding procedure was monitored by repeating the process for two separate trackfinders. This contributed ± 0.32 to the systematic error. Secondly, QED initial state radiation lowers the effective centre

of mass energy, and thus also the charge multiplicity. The reduction in $\langle n \rangle$ was estimated to be ~ 0.8 tracks at $\sqrt{s} = 35$ GeV using the QED radiative correction of Behrends and Kleiss [17] with a maximum radiative photon energy cut-off $0.98 \cdot E_{\text{beam}}$. The detector trigger and hadronic selection gave a bias of ~ 1.3 towards higher multiplicity, which was corrected for. The subtraction of the background contribution from 0.7% τ pair events and 0.9% $\gamma\gamma$ events with mean charged multiplicity of 6.0 and 7.9 respectively is accompanied by a systematic error of ± 0.13 . Differences between our Monte Carlo generators resulted in an additional systematic error of ± 0.25 , a comparison of two independent detector simulations produced ± 0.18 and the effect of the cut on the thrust axis ($|\cos \theta_{\text{thrust}}| < 0.75$) resulted in an extra systematic error of 0.07. These were added in quadrature to obtain a total systematic error of ± 0.46 [18].

The result obtained for average event charge multiplicity for $\sqrt{s} = 35$ GeV, with full corrections was

$$\langle n_{\text{ch}} \rangle = 13.31 \pm 0.03 \text{ (statistical)} \\ \pm 0.46 \text{ (systematic)}. \quad (4)$$

Following a similar procedure as in the case of whole event charged multiplicity, the result for average jets after all corrections is

$$\langle n_{\text{ch}} \rangle \text{ (average jets)} = 6.69 \pm 0.01 \text{ (statistical)} \\ \pm 0.33 \text{ (systematic)} \quad (5)$$

which can be seen to be consistent with being 1/2 of the full event charged multiplicity result in (4).

The possible bias in charged multiplicity of the b enriched sample was studied by comparing the generated charged multiplicities of Monte Carlo b jets in the whole sample and in the b -enriched sample. Since high multiplicity events are favoured in both global and jet tag modes, the contributions of residual τ pair and $\gamma\gamma$ backgrounds were negligible, in contrast to the case when we considered average jets. We therefore have to correct for this in comparing with the average jets. The tagging bias was found to be -0.19 ± 0.09 in jet charged multiplicity. The observed raw jet charged multiplicities for b enriched jets and average jets are shown in Fig. 16. The average charged multiplicity of b enriched jets, unfolded and corrected, was found to be

$$\langle n_{\text{ch}} \rangle \text{ (} b \text{ enriched jets)} = 7.44 \pm 0.15 \text{ (statistical)} \\ \pm 0.40 \text{ (systematic)}. \quad (6)$$

The uncertainty in unfolding the b jets using the matrix obtained for average jets is estimated by producing the unfolding matrix from Monte Carlo b events

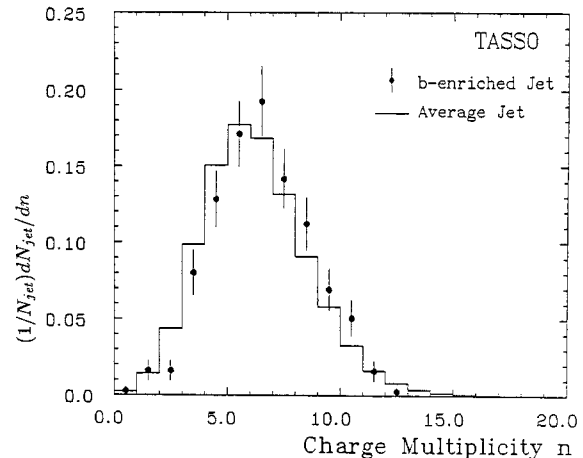


Fig. 16. Observed raw charged multiplicity in b enriched and average jets

alone. The average of the two results gives (6) while an extra systematic error of ± 0.21 is included and is equal to one half of the difference between the two unfolded results.

To extract the average charged multiplicity for b jets only, the mean charged multiplicities and the estimated flavour contents for the average hadronic jets and b enriched jets are used to form two simultaneous equations. If we hypothesise that the difference between average charge multiplicities of charm jets and uds jets is 0.5 ± 0.5 (an assumption which is consistent with published figures [19]) then we can solve these equations. We arrive at the result of

$$\langle n_{\text{ch}} \rangle \text{ (} b \text{ jets)} = 7.98 \pm 0.23 \text{ (statistical)} \\ \pm 0.68 \text{ (systematic)}. \quad (7)$$

This was after the correction of $+0.19$ for tagging bias with its uncertainty of ± 0.09 were included as systematic errors. Beside the systematic errors carried over from the result for b enriched jets, the uncertainty in the b purity of $\pm 7\%$ in the b enriched sample gives an extra contribution of ± 0.17 to the systematic error. Another systematic source comes from the uncertainty in the fraction of charm events in the b enriched sample and the assumed difference between charm jets and light flavours which amounted to ± 0.08 .

The results for the high energy data with $\langle \sqrt{s} \rangle$ of 42.1 GeV:

$$\langle n_{\text{ch}} \rangle \text{ (average jets)} = 7.44 \pm 0.03 \text{ (statistical)} \\ \pm 0.37 \text{ (systematic)} \\ \langle n_{\text{ch}} \rangle \text{ (} b \text{ jets)} = 8.51 \pm 0.50 \text{ (statistical)} \\ \pm 0.86 \text{ (systematic)}. \quad (8)$$

There are ~ 5.5 charged tracks per B decay as measured by CLEO [20], which can be compared with our result which indicates that at $\sqrt{s} \sim 35$ GeV there are 5.0 fragmentation tracks in $b\bar{b}$ events. It is therefore not surprising that some of the jet properties were rather different from those of light flavours. The Monte Carlo at $\sqrt{s} = 35$ GeV showed that a variation of $\langle z_b \rangle$ by ± 0.06 around $\langle z_b \rangle = 0.80$ corresponds to a variation of $\sim \pm 0.5$ in the average b jet charged multiplicity, which is a fairly large range considering there are only ~ 2.5 primary fragmentation tracks per jet not from B decay. The sensitivity of the multiplicity in a b jet to the b fragmentation function can be understood in the following way. The B decay provides 5.5 charged tracks on average. If the B carried only half the available energy on average, then the fragmentation tracks would be produced from half the energy of the event, 17.5 GeV. The mean charged multiplicity at $\sqrt{s} = 17.5$ GeV is about 9, half of which would appear on average in each jet. The mean b jet multiplicity would then be 10 rather than the 7.98 which we have determined.

We have used the distribution of b enriched multiplicity to determine the mean value of z_b . The raw distribution was compared with the corresponding distribution from Monte Carlo events, the multiplicity being parameterised as a function of $\langle z_b \rangle$. The distribution was well represented with a mean value of z_b of 0.89 and we obtain from the mean multiplicity $\langle z_b \rangle = 0.89 \pm 0.02$ with the error only statistical.

We can now consider the systematic errors associated with this and the largely independent measurement of $\langle z_b \rangle$ from the rapidity distribution. In the rapidity determination, we find that the systematic error is dominated by the systematic uncertainties on the tagging efficiency and from the effects of employing two different track finders [7, 21]. The result is insensitive to the details of the background from jets initiated by quarks other than b quarks. While the rapidity distribution produced by independent fragmentation is known to deviate from the data for all hadronic events at low rapidity, fitting to rapidities of greater than 1.5 gave a result which did not differ significantly from the value found using the full range of the rapidity distribution. We derive a systematic error of ± 0.03 .

The systematic error in the measurement of $\langle z_b \rangle$ in the multiplicity determination includes the uncertainty on the B decay multiplicity and a contribution from the differing effects of two track finders. Note that other contributions to the error differ from those associated with the rapidity method. The result is insensitive to the purity of the b enriched jets. We varied the number of background events due to u, d, s and

c initiated events by $\pm 40\%$ and found a variation in the extracted value of $\langle z_b \rangle$ of ± 0.01 . We note that the number of u, d, s and c jets tagged in the Lund Monte Carlo is in good agreement with the numbers from the independent jet Monte Carlo. The systematic error contains uncertainties in modelling, and the uncertainty on the B decay multiplicity. When all known effects are summed, we obtain a systematic error of ± 0.04 . This measurement is consistent with the value obtained from our rapidity distribution. We can combine the two to obtain

$$\langle z_b \rangle = 0.87 \pm 0.02 \pm 0.03$$

where the systematic error comes from the two largely independent measurements.

This result is consistent with the values determined from prompt lepton analyses. The b fragmentation is very hard, as predicted on theoretical grounds [12, 22] and as elsewhere measured [16].

7 Test of flavour independence of α_s

The flavour independence of α_s can best be tested by measuring the ratio of α_s for different flavours and so cancelling many systematic effects. Note that the α_s measured from all hadronic events is influenced only very little by the b flavoured component. We choose to use the asymmetry (AEEC) in the Energy-Energy Correlation (EEC) [23] for this measurement.

The normalised EEC is defined as

$$\begin{aligned} \frac{1}{\sigma_0} \frac{d\Sigma(\cos \chi)}{d \cos \chi} &= f(\cos \chi) \\ &= \frac{1}{N} \sum_{\text{Events } i, j} \sum \frac{E_i \cdot E_j}{W_{\text{vis}}^2} \delta(\cos \chi - \cos \chi_{i,j}) \end{aligned} \quad (9)$$

where $\chi_{i,j}$ is the angle between two particles i and j with energies E_i and E_j . W_{vis} is the total visible energy in an event. The summation is extended over all pairs i, j of particles in an event including the case $i=j$, and over all events N . The normalisation is therefore

$$\int f(\cos \chi) d \cos \chi = 1. \quad (10)$$

Most of the effects of 2 jet fragmentation and centre of mass energy dependence can be removed by considering the asymmetry of EEC:

$$A((\cos \chi) = f(\cos(\pi - \chi)) - f(\cos \chi)). \quad (11)$$

The remaining effects due to fragmentation of 2 jet events near $|\cos \chi| \sim 1$ can be further suppressed by constraining the fits to obtain α_s from the region

Table 5. Tagging efficiencies of different flavour/parton topology in global-mode

Monte Carlo flavours	Tagging efficiency	
	2 jets	3 or 4 jets
$b\bar{b}$	$19.6 \pm 0.4\%$	$11.1 \pm 0.5\%$
$c\bar{c}$	$1.8 \pm 0.2\%$	$1.5 \pm 0.2\%$
uds	$0.5 \pm 0.1\%$	$0.5 \pm 0.1\%$

$|\cos \chi| < 0.7$ of the EEC asymmetry. The detailed discussion of the merits of EEC, especially its asymmetry, can be found elsewhere [24, 25].

7.1 Data and Monte Carlo samples

All 1986 hadronic data at $\sqrt{s} = 35$ GeV are used to obtain the α_s measurement for the average of all flavours, while the b enriched sample, used for the measurement of $\alpha_s(b)$, was isolated using the global-mode. The global-mode tag gives a sample of 516 events with an estimated $b\bar{b}$ purity of $68 \pm 7\%$. To check possible biases in the tagging procedure, the efficiencies for accepting 2 jet events and 3 or 4 jets events, were studied in Monte Carlo events and are shown in Table 5.

Since the results of α_s measurements are very sensitive to the QCD matrix element calculation and fragmentation models used, we reiterate here the important aspects of the Monte Carlo. The Monte Carlo used an extended FKSS 2nd order QCD matrix element [11] with an (ε, δ) cut of $(0.1, 40^\circ)$, together with an independent jet fragmentation scheme where gluons were fragmented in the same way as quarks and the energy-momentum conservation scheme was according to the Monte Carlo of Ali et al. [26].

7.2 Results and systematic effects

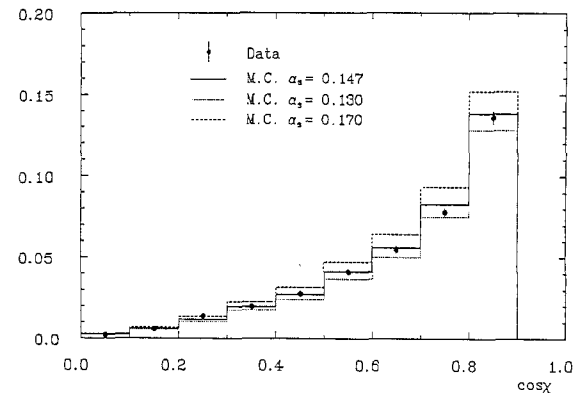
The EEC asymmetry distribution was fitted in the region $|\cos \chi| < 0.7$, giving the result

$$\alpha_s(\text{average hadrons}) = 0.147 \pm 0.004 \text{ (statistical only)} \quad (12)$$

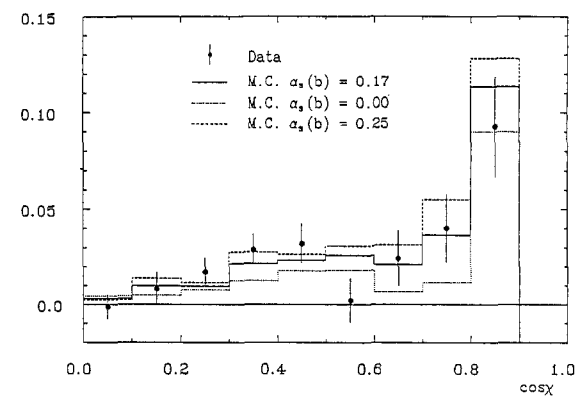
with a $\chi^2/\text{d.o.f.}$ of 2.0/6. With the fitting range fixed to $|\cos \chi| < 0.6$ and then $|\cos \chi| < 0.8$, the result in α_s changed by ± 0.004 . The AEEC distribution with the above α_s value for the Monte Carlo is compared with data in Fig. 17.

This result is consistent with a more comprehensive and systematic study of energy energy correlations in the TASSO data [25]. For our present purposes, we only aim to extract the the ratio of $\alpha_s(b)$

EEC Asymmetry

**Fig. 17.** EEC asymmetry distribution of average hadrons

EEC Asymmetry

**Fig. 18.** EEC asymmetry distribution of b enriched sample

to $\alpha_s(\text{all})$ and have not attempted to get the best absolute value. The EEC asymmetry distribution of the b enriched sample was then also fitted in the region $|\cos \chi| < 0.7$, but fixing the α_s value for $udsc$ flavours to that of the average of all hadrons as in (12) and only allowing $\alpha_s(b)$ to vary. We find:

$$\alpha_s(b) = 0.172 \pm 0.073 \text{ (statistical only)} \quad (13)$$

with a $\chi^2/\text{d.o.f.}$ of 7.5/6. The measured value of α_s changed by ± 0.02 in varying the fitting range in the same way as for the average hadrons. Tagging biases for 3 or 4 jet events are taken care of during fitting. The AEEC distribution for the b enriched sample with the best fit of α_s values for the Monte Carlo is compared with data in Fig. 18.

The most important systematic errors are flavour-dependent. The most prominent of these is due to the present rather poor knowledge of the b fragmentation function. The standard Monte Carlo used the Peterson function with $\varepsilon_b = 0.010$, corresponding to $\langle z_b \rangle = 0.80$. As mentioned, we also generated Monte

Carlo b events with ε_b of 0.003 and 0.03 respectively which represent the two extremes of experimental measurement results, and were processed at the generator level only. This study showed that with a harder b fragmentation (with $\langle z_b \rangle = 0.86$) the measured value of the ratio $R = \alpha_s(b)/\alpha_s(\text{average})$ increased by 0.20 and with the softer b fragmentation, it decreased by 0.20. This will be seen to be the major systematic error.

The QCD matrix element calculations with full 2nd order corrections for 3 parton final states assumed all quarks were massless. Since no full second order matrix element calculation with quark masses included is available, we compared the cases of partial second order calculations (no virtual corrections for 3 parton final states) with and without quark masses in the matrix elements. The study of AEEC distributions at the Monte Carlo generator level showed that the inclusion of masses would only result in an effective increase of measured R of 0.04 and is therefore negligible.

Varying the assumed α_s value of the $udsc$ background by ± 0.01 [27] in the fit to the b enriched sample resulted in a change of ± 0.07 in R . Varying the assumed b purity by $\pm 10\%$ resulted in a change of ± 0.07 in R . The flavour-dependent systematic errors in R total ± 0.27 .

All other known sources of systematic error are flavour blind, at least when compared with the magnitude of that associated with the uncertainty in the b fragmentation function. We attribute a collective systematic error of 10% on the ratio $\alpha_s(b)/\alpha_s(\text{average})$ to account for all effects due to different fragmentation models and thereby arrive at the final result

$$\frac{\alpha_s(b)}{\alpha_s(\text{average})} = 1.17 \pm 0.50 \pm 0.28. \quad (14)$$

The strong coupling strength of the b quark is consistent with being the same as the other flavours.

8 Summary

We have demonstrated a new technique which is shown to have a high efficiency in obtaining a relatively pure sample of $b\bar{b}$ hadronic events. This is the first occasion the long lifetime of the B hadrons was used for the purpose.

We have studied the fragmentation properties of the b quark and made comparison with average hadronic events in which the b flavour only make up $\sim 10\%$. The gross properties of b jets are very similar to those from average jets, despite the fact that most particles arise from B decay rather than fragmentation. b jets have a slightly higher multiplicity and are slightly softer and more spherical than the average

jet. All these differences can be understood in terms of a mean z_b of 0.87 and are well reproduced by Monte Carlo. The multiplicity and rapidity distributions have been used to make two new determinations of the mean value of z_b and these are independent of a hard lepton tag. We find

$$\langle z_b \rangle = 0.87 \pm 0.02 \pm 0.03$$

which is in agreement with both previous determinations and theoretical predictions. Our studies have verified the validity of current models of jets initiated by the b quark.

We have made the first measurement of the strong coupling constant to b quarks and find it is consistent with being identical to that of the light quarks.

Acknowledgements. We wish to thank the PETRA machine group and the DESY computer centre for their excellent support, particularly in the high luminosity runs of 1986. Those of us from outside DESY thank the DESY Directorate for their hospitality.

References

1. For more details on the tagging method and analysis on high energy data, see: Su Dong: Ph.D. Thesis, Imperial College, London Univ. (1987); RAL-T-061
2. DELCO Coll. M. Sakuda et al.: Phys. Lett. 152B (1985) 399; Mark II Coll. P.C. Rowson et al.: Phys. Rev. Lett. 54 (1985) 2580
3. TASSO Coll. R. Brandelik et al.: Phys. Lett. 83B (1979) 261; TASSO Coll. M. Althoff et al.: Z. Phys. C – Particles and Fields 22 (1984) 13
4. D.M. Binnie et al.: Nucl. Instrum. Methods 228 (1985) 267
5. H. Boerner et al.: Nucl. Instrum. Methods 176 (1980) 151
6. TASSO Coll. M. Althoff et al.: Z. Phys. C – Particles and Fields 22 (1984) 307
7. A.J. Campbell: Ph.D. Thesis, Imperial College, London Univ. (1983), RL-HEP/T/117
8. D.H. Saxon: Nucl. Instrum. Methods A234 (1985) 258
9. P. Avery: CLNS-84/608 (1984)
10. TASSO Coll. M. Althoff et al.: Z. Phys. C – Particles and Fields 26 (1984) 157
11. K. Fabricius et al.: Phys. Lett. 97B (1980) 431; Z. Phys. C – Particles and Fields 11 (1982) 315
12. C. Peterson et al.: Phys. Rev. D27 (1983) 105
13. T. Sjöstrand: Comp. Phys. Commun. 39 (1986) 3
14. TASSO Coll. W. Braunschweig et al.: DESY 88-034, submitted to Z. Phys. C
15. TASSO Coll. M. Althoff et al.: Phys. Lett. 149B (1984) 524
16. MAC Coll. E. Fernandez et al.: Phys. Rev. Lett. 50 (1983) 2054; Mark J Coll. B. Aveda et al.: Phys. Rev. Lett. 51 (1983) 443; TASSO Coll. M. Althoff et al.: Z. Phys. C – Particles and Fields 22 (1984) 219; TASSO Coll. M. Althoff et al.: Phys. Lett. 146B (1984) 443; JADE Coll. W. Bartel et al.: Z. Phys. C – Particles and Fields 33 (1987) 339; Mark II Coll. R.A. Ong et al.: Phys. Rev. Lett. 60 (1988) 2587
17. F.A. Behrends, R. Kleiss: Nucl. Phys. B177 (1981) 237; Nucl. Phys. B178 (1981) 141

18. TASSO Coll. W. Braunschweig et al.: DESY 88-046, submitted to Z. Phys. C
19. Mark II Coll. P.C. Rowson et al.: Phys. Rev. Lett. 54 (1985) 2580; HRS Coll. P. Kesten et al.: Phys. Lett. 161 B (1985) 412
20. CLEO Coll. M. Alam et al.: Phys. Rev. Lett. 49 (1982) 357; CLEO Coll. R. Giles et al.: Phys. Rev. D 30 (1984) 2279
21. D. Cassel, H. Kowalski: Nucl. Instrum. Methods 185 (1981) 235
22. J. Bjorken: Phys. Rev. D 17 (1978) 171; M. Suzuki: Phys. Lett. 71 B (1978) 139; M.G. Bowler: Z. Phys. C – Particles and Fields 11 (1981) 169; B. Anderson et al.: Z. Phys. C – Particles and Fields 20 (1983) 317
23. C.L. Basham et al.: Phys. Rev. Lett. 41 (1978) 1585
24. A. Ali, F. Barreiro: Nucl. Phys. B 236 (1984) 269
25. TASSO Collab. M. Althoff et al.: Z. Phys. C – Particles and Fields 36 (1987) 349
26. A. Ali et al.: Phys. Lett. 93 B (1980) 155
27. G. Rudolf: DESY 84-057 (1984)